

A LENA Instrument onboard BepiColombo and Chandrayaan-1

Yoichi Kazama¹, Stas Barabash², Martin Wieser², Kazushi Asamura³, and Peter Wurz⁴

¹*Institute of Aerospace Technology, Japan Aerospace Exploration Agency, Tsukuba, Ibaraki, Japan*

²*Swedish Institute of Space Physics, Kiruna, Sweden*

³*Institute of Space and Astronautical Science, Japan Aerospace Exploration Agency, Sagami-hara, Kanagawa, Japan*

⁴*University of Bern, Bern, Switzerland*

ABSTRACT

Low-energy neutral atom (LENA) observations bring us important information on particle environments around planetary objects such as Mercury and the Moon. In this paper, we report on a new development of a LENA instrument of light weight (~2 kg) for planetary explorations. The instrument is capable of energy and mass discrimination with a large sensitivity by utilizing surface ionization followed by an electrostatic analyzer and a time-of-flight velocity spectrometer. The performance of the instrument is investigated by numerical simulations. This enables us to obtain detailed performance characterization of LENA measurements by the instrument. We also made trajectory tracing of photons entering the instrument to examine photon rejection capability. The simulations show that the energy range is from ~10 eV to >3.3 keV and the angular resolutions are 10 deg × 25 deg for 25-eV LENAs, which are sufficient for planetary LENA observations. Laboratory tests of a prototype model of the instruments developed with this study are now ongoing. According to the initial tests, the measurement principle of the instrument has been verified. This LENA instrument has been selected for both the Indian Moon exploration mission Chandrayaan-1 and the European-Japanese Mercury exploration mission BepiColombo.

INTRODUCTION

Low-energy neutral atoms (LENAs) are created by interactions of energetic ions with the planetary surface and exospheric neutral gases. The solar wind and/or energetic magnetospheric ions hit the surfaces of Mercury and the Moon, and LENAs are produced through sputtering of the surface materials, or back-scattering of the precipitating ions. Charge exchange of the ions with exospheric gases is also a process to create LENAs. LENA observation is important to make comprehensive understanding of the particle environments of Mercury and the Moon.

The Swedish Institute of Space Physics (Institutet för rymdfysik; IRF) is now developing a LENA instrument in cooperation with Institute of Space and Astronautical Science (ISAS) in Japan, and University of Bern (UBe) in Switzerland. The instrument has been selected for the Indian Moon exploration mission Chandrayaan-1 (Bhardwaj *et al.*, 2005) and the European-Japanese Mercury exploration mission BepiColombo. In this paper, we briefly report expected performances of the instrument by numerical simulations. For details, refer to Kazama *et al.* (2007).

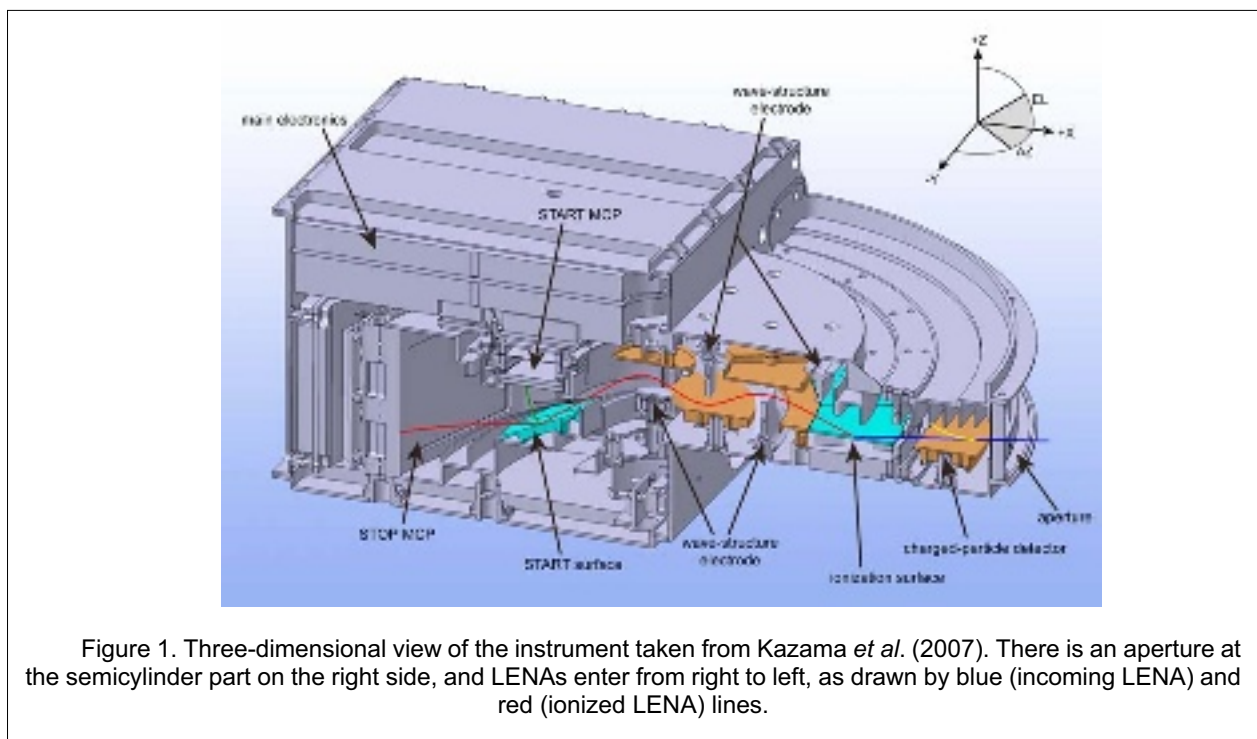
DESIGN OF THE INSTRUMENT

Figure 1 illustrates a cross-sectional view of the whole instrument in three dimensions. The instrument consists of a sensor and electronics. The sensor has two parts of semicylinder-like shape, both of which are concentric. The aperture opens on the front cylinder part (right-hand side in the figure). The field of view is fan-shaped, which enables us to scan the whole sky by spin motion of a spin-stabilized satellite, or to scan the planetary surface by orbital motion of a low-altitude three-axis-stabilized satellite.

Inside the sensor, there are four components: the charged-particle deflector, the ionization surface, the wave structure (in the front cylinder part), and the time-of-flight (TOF) part (in the rear cylinder part). An entering LENA through the aperture first passes through the charged-particle deflector where ambient plasmas are swept out by an electrostatic field. The charged-particle deflector also defines the field-of-view in elevation angle by its baffle vanes and the deflection electrode.

Hitting on the ionization surface, LENAs are positively ionized with a certain probability (e.g. Wieser *et al.*, 2002). The positively-ionized particle is then guided through the wave structure where the ionized particles are electrostatically guided up and down. The wave structure makes electrostatic energy analysis, meaning that a setting of electrode voltages defines an energy range of the particles which can go through the wave structure. The upper and lower walls of the wave structure have fine serrations on their surfaces and are blackened with CuS coating to suppress photon reflection.

After the wave structure, the particles are accelerated by the lens electrodes to hit on the START surface in the TOF part. Collision of a particle with the START surface creates secondary electrons, which produce a start signal at the START MCP (micro-channel plate) for a TOF measurement. The particles are then scattered after hitting the surface, and are finally detected by the STOP MCP to generate stop signals. By measuring a TOF between the start and stop signals, the velocity of the particle is acquired. The START MCP has seven sector anodes to cover ± 75.25 deg, which are used to determine azimuth angles of LENAs.



ESTIMATION OF INSTRUMENT PERFORMANCE

In this section, results of particle-tracing simulations are described. Since the instrument employs surface scattering to ionize neutrals and to emit secondary electrons, it is needed to include surface-scattering behaviors of particles in order to calculate realistic trajectories of particles.

We have developed a new computer code for calculations of the electric fields and particle trajectories in three dimensions. Combining a surface-scattering model of particles and a secondary electron emission model (either not mentioned in this report, see Kazama *et al.* (2007) for the details), this code enables us to calculate full trajectories of LENAs from the aperture to the detector, including particle's ionization, scattering, and secondary electron release. The code can also trace trajectories of photons with a surface reflection model of photons.

Performance of Photon Rejection

Rejection of photons is one of the keys of this instrument, since MCPs are sensitive to photons as well as particles. The rejection ratio of photons is obtained by a numerical photon-tracing simulation. About photon reflection on a wall, diffuse reflection with a reflection coefficient of 10^{-2} (Zurbuchen *et al.*, 1995) is assumed except for the ionization and the START surfaces, for which specular reflection with a reflection coefficient of 10^{-1} is assumed because these surfaces are neither CuS-blackened nor perfectly specular. This means that these surfaces must have a coefficient between 10^{-2} and 10^0 . Thus, 10^{-1} is a good assumption as the reflection coefficient.

The results of the simulations indicate that the photon count rates of the START MCP and STOP MCP at the Mercury orbit are estimated to be 0.4 count/sec and 60 count/sec, respectively, for the solar H Ly- α (121.6 nm) radiation. The difference of the count rates comes from the positions of the STOP MCPs, which are placed toward the aperture of the instrument. Thus, assuming 1000 nsec of the TOF window, the coincidence count rate due to photons is estimated to be $0.4 \times 60 \times 1000 \times 10^{-9} \sim 2 \times 10^{-5}$ count/sec. Since the count rate of ~ 25 -eV LENAs is expected to be more than 0.1 /sec as will be discussed below, the count rate due to photons is significantly lower than that of LENAs, indicating that photons do not affect LENA measurements.

Performance of Ion Rejection

Ambient ions must be swept out by the charged-particle deflector before reaching the ionization surfaces. Once ambient ions hit the surfaces, it is not possible to distinguish ionized neutrals from the ions. The rejection performance of ambient ions was estimated by particle-tracing simulations. Here the transmission ratio is defined as a ratio of the number of ions hitting the ionization surface to the number of all the randomly-injected ions. According to Wieser *et al.* (2002), roughly $>90\%$ of ions are neutralized on the surface and are not detected. This low ionization ratio is not included in the simulation for taking the worst case into account.

According to the results of the simulations with the deflection electrode voltage of 5 kV, the transmission ratio is approximately 4×10^{-5} at 14 keV, and none of 10^6 particles reaches the surfaces at 13 keV. Therefore, the cut-off energy is between 13 and 14 keV, ~ 13.5 keV in conclusion.

Performance of LENA Measurement

Sensitivity of LENA Detection

Overall sensitivities for LENAs were calculated by the computer simulations. Here an overall sensitivity includes all factors that reduce detection possibility: two mesh transmittances of $(90\%)^2$, ionization efficiency of 10%, secondary electron creation of 100%, surface reflection ratio of $(50\%)^2$, LENA's MCP detection efficiency of 60%, and electron's MCP detection efficiency of 100%. These factors sum up to 1.22%.

According to the results, the sensitivities are of the order of $10^{-2} \text{ cm}^2 \text{ sr eV}$ for 25-eV LENAs, and $10^{-1} \text{ cm}^2 \text{ sr eV}$ for 3300-eV LENAs. By Lukyanov *et al.* (2004), LENA fluxes at Mercury are estimated at $10^1 - 10^3$ /sec $\text{cm}^2 \text{ sr eV}$ in the energy range of 10 – 100 eV. Hence, LENA count rates of 0.1 – 10 /sec can be expected in a 25-eV energy range, which is sufficient to fulfill scientific goals. In the case of the Moon, expected fluxes of >10 -eV LENA are $\sim 10^3 - 10^5 \text{ cm}^2 \text{ sr eV}$, according to Futaana *et al.* (2006). Therefore, even higher LENA count rates can be expected at the Moon.

Field-of-View and Angular Resolution

For LENA mapping, a wide field-of-view (FOV) and fine angular resolution are needed. Both the FOV and resolution in elevation angle are 10 deg FWHM, which is defined geometrically by the collimator of the charged-particle deflector. About the azimuth-angle direction, the simulation results indicate that the FOV is ± 75 deg for 25-eV LENAs and ± 63 deg for 3300-eV LENAs, and the resolution is 25 – 30 deg for both the energy cases. The degradation of the FOV is caused by the distorted electric field at the center of the sensor part, in which azimuth directions of particles are more biased toward the center, according to the detailed analysis in Kazama *et al.* (2007). Obviously, finer angular resolution needs higher detection sensitivity to keep statistical accuracy. These FOVs and resolutions are a good compromise for successful LENA measurement.

Mass Resolution

Calculated TOF spectra for major species such as H, O, Na, K, Fe in the 25-eV case show that the mass resolution $m/\Delta m$ is 3 or less, meaning that the instrument does not distinguish between heavy species, for example, Na from Mg, K from Ca. However, abundances of mass groups, such as Na/Mg group and K/Ca group, can still be

obtained from TOF distributions. Considering the limitations on the instrument, we conclude that this mass resolution is satisfactory from the scientific point of view.

Energy Range and Resolution

The energy range of the instrument is $\sim 10 - 3300$ eV, which is determined by the limitation of a high-voltage power supply. Energy selection is made by changing voltages of the electrodes in the wave structure. According to the simulations, the energy resolution is $\sim 70\%$ for 25-eV LENAs and $\sim 110\%$ for 3300-eV LENAs. It is noted that the energy resolution is a function of a tuned energy because particles are accelerated before energy selection.

INITIAL RESULT WITH THE PROTOTYPE MODEL

After these simulations were made, a prototype model of the instrument was manufactured to examine the actual performances in the laboratory. The photograph of the model is shown in Figure 2. Now laboratory tests with the prototype are being made at IRF. Figure 3 shows a TOF spectrum taken from the initial test. A clear peak is seen at approximately 340 nsec, which is consistent with the 1.3-keV H_2O^+ beam. This result demonstrates that the TOF measurement of the instrument works fine. It is noted that a small peak at about 200 nsec is due to sputtered particles initially stayed on the START surface.



Figure 2. Photograph of the prototype of the instrument. The collimator and the wave-type structure are on the left-hand side, and the TOF part, the MCPs and the front-end electronics are inside of the box on the right side.

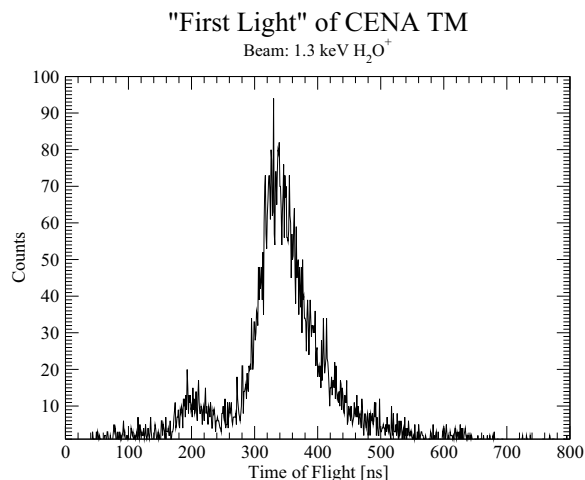


Figure 3. TOF spectrum taken with the prototype model of the instrument. The test was made in the calibration facility of IRF by using a H_2O^+ beam. One can see that a clear peak of the beam, which shows that TOF measurement works fine.

SUMMARY

We developed a new instrument to measure low-energy neutral atoms (LENAs) in planetary explorations, and the performances of the instrument have been studied by computer simulations of full trajectory tracing. The performances of the LENA instrument are summarized in Table 1.

This newly-developed LENA instrument covers wide energy range from ~ 10 eV to >3.3 keV, corresponding to energies of LENAs sputtered from planet surfaces and charge-exchanged or back-scattered from energetic ions. The angular resolutions are 10 deg in elevation and 25 – 30 deg in azimuth, and the resolutions are enough for LENA imaging observation. The instrument is capable of discriminating major mass groups of LENAs produced from the surfaces of Mercury and the Moon. This capability enables us to study sources and generation processes of LENAs. Furthermore, it should be emphasized that these performances are achieved under a 2-kg limitation of total instrument mass. Light weight is crucial in planetary exploration missions. Manufacturing of a prototype of the instrument has been completed, and laboratory tests are now ongoing at IRF. According to preliminary tests, a TOF spectrum of a H₂O beam was obtained, which demonstrates that the TOF measurement works well.

This LENA instrument has been selected for both the Indian Moon exploration mission Chandrayaan-1 and the European-Japanese Mercury exploration mission BepiColombo.

Table 1. Summary of the instrument performances.

Item	Figure	Unit	Remark
Weight	2	kg	overall (sensor, electronics, etc.)
Sensitivity	$\sim 10^{-2}$	cm ² sr eV	per channel, for 25-eV LENA
	$\sim 10^{-1}$	cm ² sr eV	per channel, for 3300-eV LENA
Energy range	$\sim 10 - >3300$	eV	
Energy resolution	~ 70	%	for 25-eV LENA
	~ 110	%	for 3300-eV LENA
Field of view	~ 10	deg	elevation, FWHM
	$\sim +/-75$	deg	azimuth, for 25-eV LENA
	$\sim +/-63$	deg	azimuth, for 3300-eV LENA
Angular resolution	~ 10	deg	elevation, FWHM
	$\sim 25 - \sim 30$	deg	azimuth, FWHM
Mass resolution	$< \sim 3$		capable of discriminating mass groups
Power consumption	~ 3.3	W	
Data production	2	Kbps	

REFERENCES

- Bhardwaj, A., S. Barabash, Y. Futaana, Y. Kazama, K. Asamura, D. McCann, R. Sridharan, M. Holmström, P. Wurz, and R. Lundin, Low energy neutral atom imaging on the Moon with the SARA instrument aboard Chandrayaan-1 mission, *J. Earth Sys. Sci.*, 114, 749–760, 2005
- Futaana, Y., S. Barabash, M. Holmström, and A. Bhardwaj, Low energy neutral atoms imaging of the Moon, *Planet. Space Sci.*, 54, 132–143, 2006
- Kazama, Y., S. Barabash, M. Wieser, K. Asamura, and P. Wurz, Development of an LENA Instrument for Planetary Missions by Numerical Simulations, *Planet. Space Sci.*, 55, 1518–1529, 2007
- Lukyanov, A., S. Barabash, and M. Holmström, Energetic neutral atom imaging of Mercury's magnetosphere 3. Simulated images and instrument requirements, *Adv. Space Res.*, 33, 1890–1898, 2004
- Wieser, M., P. Wurz, K. Brüning, and W. Heiland, Scattering of atoms and molecules off a magnesium oxide surface, *Nucl. Instr. Methods Phys. Res. B*, 192, 370–380, 2002
- Zurbuchen, T., P. Bochsler, and F. Scholze, Reflection of ultraviolet light at 121.6nm from rough surfaces, *Opt. Eng.*, 34(5), 1303–1315, 1995